

On the resolution power of Fourier extensions for oscillatory functions

Ben Adcock* and Daan Huybrechs†

Abstract

Functions that are smooth but non-periodic on a certain interval have only slowly converging Fourier series, due to the Gibbs phenomenon. However, they can be represented accurately by a Fourier series that is periodic on a larger interval. This is commonly called a Fourier extension. Fourier extensions have been mostly used to solve PDE's on complicated domains, by embedding the domain into a larger bounding box and extending all functions involved to Fourier series on that box, thereby enabling fast FFT-based algorithms. Fourier extensions have also been employed to resolve the Gibbs-phenomenon for non-periodic functions.

In this paper we describe, analyze and explain the observation that Fourier extensions also have excellent resolution properties for representing oscillatory functions. The *resolution power*, or required number of degrees of freedom per wavelength, depends on a user-controlled parameter and varies between 2 and π . The former value is optimal and is achieved for example by classical Fourier series for periodic functions. The latter value is the resolution power of polynomials. In addition, we also introduce and analyze a new numerical method for computing Fourier extensions, which improves on previous approaches.

1 Introduction

In many physical problems, one encounters the phenomenon of oscillation. When approximating the solution to such a problem with a given numerical method, this naturally leads to the question of resolution power. That is, how many degrees of freedom are required in a given scheme to resolve such oscillations? Whilst it may be impossible to answer this question in general, important heuristic information about a given approximation scheme can be gained by restricting ones interest to certain simple classes of functions (e.g. complex exponentials for problems in bounded intervals).

Resolution power represents an *a priori* measure of the efficiency of a numerical scheme for a particular class of problems. Approximations with low resolution power require more degrees of freedom, and hence increased computational cost, before the onset of convergence. Conversely, schemes with high resolution power resolve oscillations with far fewer degrees of freedom, resulting in a decreased computational expense.

*Department of Mathematics, Simon Fraser University, Canada (ben_adcock@sfu.ca)

†Department of Computer Science, Katholieke Universiteit Leuven, Belgium (daan.huybrechs@cs.kuleuven.be)

Consider the case of the unit interval $[-1, 1]$ (the primary subject of this paper). Here, one typically studies the question of resolution via the complex exponentials

$$f(x) = \exp(i\omega\pi x), \quad \omega \in \mathbb{R}. \quad (1)$$

To this end, let $\phi_n(f)$, $n = 1, 2, \dots$ be a sequence of approximations of the function $f(x) = \exp(i\pi\omega x)$, which converges to f as $n \rightarrow \infty$. Say that, for a given ω , the asymptotic convergence to f sets in once n exceeds a critical value n^* . We refer to the ratio $r = \frac{n^*}{\omega}$ as the *resolution constant* of the approximation scheme. Loosely speaking, this quantity corresponds to the required number of degrees of freedom per wavelength, a common concept in the literature on oscillatory problems. In particular, a given scheme has high (respectively low) resolution power if it has small (large) resolution constant. Note, however, that r is not guaranteed to actually be a constant, nor is this definition entirely rigorous. We forgo a more formal definition for the sake of clarity. In the schemes we consider in this paper, r will always be a constant and its meaning clear.

With little doubt, the approximation of a smooth, periodic function via its truncated Fourier series is one of the most effective numerical methods known. Fourier series, when computed via the FFT, lead to highly efficient, stable methods for the numerical solution of a large range of problems (in particular, PDE's with periodic boundary conditions). A simple argument leads to a resolution constant of 2 in this case (for periodic oscillations), with exponential convergence occurring once the number of Fourier coefficients exceeds 2ω .

However, the situation is altered completely once periodicity is lost. The slow pointwise convergence of the Fourier series of a nonperiodic function, as well as the presence of unpleasant $\mathcal{O}(1)$ Gibbs oscillations near the domain boundaries, means that nonperiodic oscillations cannot be resolved by such an approach. A standard alternative is to approximate smooth but nonperiodic functions via a sequence of orthogonal polynomials (Chebyshev polynomials, for example). Such approximations possess exponential convergence, without periodicity, yet the resulting resolution constant increases to precisely the value π , making such an approach clearly less than ideal.

Another collection of commonly used methods arise from the desire to reconstruct a function directly from its Fourier coefficients, whether via re-expanding in a sequence Gegenbauer polynomials [16, 17], or by smoothing the function by implicitly matching its derivatives at the domain boundary [13]. Whilst the latter retains a resolution constant of 2, it only yields algebraic convergence of a finite order, and suffers from severe ill-conditioning. Conversely, the Gegenbauer reconstruction procedure offers exponential convergence, but with a significant deterioration in the resolution power [15].

Although many of these methods have proved successful in a wide variety of applications, none is evidently optimal for resolving oscillatory phenomena. The intent of this paper is to study a different approach for this problem, the so-called *Fourier extension* method [5, 9, 19]. As we shall show, this method involves a user-determined parameter $T \in (1, \infty)$ that allows for continuous variation of the resolution constant from the value 2 (in the limit $T \rightarrow 1$), the figure corresponding to Fourier series, to π ($T \rightarrow \infty$), the value obtained by orthogonal polynomial expansions. Thus, the Fourier extension method is highly suitable for problems with oscillations at moderate to high frequencies.

The use of Fourier extensions to resolve oscillatory functions is superficially quite similar to the Kosloff–Tal–Ezer mapping (see [21], [4, chpt 16.9] and references therein, and more recently, [18]) for improving the severe time-step restriction inherent in Chebyshev spectral methods. Such an approach also improves the very much related property of resolution power. In this approach, one replaces the standard Chebyshev interpolation nodes with a sequence of mapped points, and expands in a nonpolynomial basis defined via the particular mapping. Roughly speaking, with Fourier extensions, the situation is reversed. Rather than specifying interpolation nodes, one specifies the particular basis (i.e. the Fourier basis) and chooses an appropriate collection of nodes that gives rapidly convergent expansions and good resolution properties. This feature leads to an obvious application of Fourier extensions in the numerical solution of PDE's. Fourier series diagonalise constant coefficient differential operators, making them well-suited for such problems. The use of Fourier extensions (or similar versions) in this context has been explored in [6, 23] and, more recently, in [8, 22].

We describe the topics of resolution power and Fourier extensions in more detail below. Before doing so, a word about terminology in order to avoid confusion. We will refer to the following three types of convergence of an approximation f_n to a given function f . We say that f_n converges *algebraically fast* to f at rate k if $\|f - f_n\| = \mathcal{O}(n^{-k})$ as $n \rightarrow \infty$. Conversely, f_n converges *spectrally fast* to f if the error $\|f - f_n\|$ decays faster than any algebraic power of n^{-1} , and *exponentially fast* if there exists some constant $\rho > 1$ such that $\|f - f_n\| = \mathcal{O}(\rho^{-n})$ for all large n .

1.1 Resolution power

The question of resolution power of Fourier series and Chebyshev polynomial expansions was, arguably, first studied rigorously by Gottlieb and Orszag [14, p.35]. Therein the figures of 2 and π respectively were derived, the latter being generalized to arbitrary Gegenbauer polynomial expansions in [15] (in Section 3 we provide an alternative proof, valid for almost any orthogonal polynomial system (OPS)). Resolution was also discussed in [4, chpt. 2], where, aside from Fourier and Chebyshev expansion, the extremely poor performance of finite difference schemes was noted.

The Gegenbauer reconstruction technique introduced by Gottlieb et al [16, 17] was shown in [15] to have poor resolution properties (see also [3]). To mitigate this effect, a domain decomposition approach was considered in [3], but with only algebraic rate of convergence.

1.2 The Fourier extension method

In this section we briefly recap the Fourier extension method as presented in [5, 9] and, in particular, [19].

Fourier series are eminently suitable for approximating smooth and periodic functions. A potential means to recover a highly accurate Fourier representation of a nonperiodic function $f : [-1, 1] \rightarrow \mathbb{R}$ is to seek to extend f to a periodic function g defined on a larger domain $[-T, T]$ and compute the Fourier series of g . Unfortunately, unless f is itself periodic, no periodic extension g will be

analytic, and hence only spectral convergence can be expected. Preferably, for analytic f , we seek an approximation that converges exponentially fast.

To remedy this situation, rather than computing an extension g , it was proposed in [5, 9] to directly compute a Fourier representation of f on the domain $[-T, T]$ via the so-called *Fourier extension problem*:

Problem 1.1. *Let G_n be the space of $2T$ -periodic functions of the form*

$$g \in G_n : g(x) = \frac{a_0}{2} + \sum_{k=1}^n a_k \cos \frac{\pi}{T} kx + b_k \sin \frac{\pi}{T} kx. \quad (2)$$

The Fourier extension of f to the interval $[-T, T]$ is the solution to the optimization problem

$$g_n := \arg \min_{g \in G_n} \|f - g\|_{L^2_{[-1,1]}}. \quad (3)$$

As numerically observed in [5, 9], the convergence of g_n to f is truly exponential, provided f is analytic. This apparent contradiction can be explained by noting that the sequence of approximations g_n do not converge to a fixed function g outside $[-1, 1]$ (see [5, 19]).

When $T = 2$, these observations were confirmed by the analysis presented in [19]. A pivotal role is played by the map

$$y = \cos \frac{\pi}{2} x. \quad (4)$$

The importance of this map is that it transforms the trigonometric basis functions that span the space G_n into polynomials in y . In this setting, Problem 1.1 reduces simply to the computation of expansions in a suitable basis of nonclassical orthogonal polynomials, as the least squares criterion corresponds exactly to an orthogonal projection in a particular weighted norm. Well-known results in the field of orthogonal polynomials can then be used to establish convergence properties of the Fourier extension. We recall this analysis in greater detail further on in §2, along with its generalization to general T .

The map (4) demonstrates the close relationship that exists between Fourier series and polynomials. Note the similarity to the classical Chebyshev map $x = \cos \theta$ that turns Chebyshev polynomials into trigonometric basis functions. Compared to Chebyshev expansions, however, it is interesting to observe that the roles of polynomials and trigonometric functions are interchanged. The Chebyshev expansion of a given function f is a polynomial approximation, which is equivalent to the Fourier series of a related function. The Fourier extension of a function on the other hand is a trigonometric approximation, which is equivalent to the polynomial expansion of a related function. In that sense, Fourier extensions and Chebyshev expansions are dual to each other.

One-dimensional Fourier extensions have been employed to overcome both the Gibbs phenomenon in standard Fourier expansions [5] and the Runge phenomenon in equispaced polynomial interpolation [7]. Application to surface parametrisations was explored in [9]. Similar ideas (typically referred to as *Fourier embeddings*) were proposed in [6, 23] to solve certain BVP's. More recently, a method was developed in [8, 22] to solve time-dependent PDE's in complex geometries. This was based on a similar, but not identical way of obtaining one-dimensional Fourier extensions, in combination with an alternating

direction technique to handle general domains. Interestingly, it is shown and emphasized in [22] (see also [2]) that this method leads to an absence of dispersion errors (or pollution errors) – another beneficial property for wave simulations shared with classical Fourier series, and very much related to resolution power.

Having said this, to the best of our knowledge, the resolution properties of Fourier extensions have not yet been rigorously explored.

1.3 Key results and outline

The main result of this paper is that the resolution constant $r = r(T)$ of the exact Fourier extension satisfies

$$r(T) \leq T\sqrt{2 - 2c(T)}, \quad T \in (1, \infty),$$

where for ease of notation we have defined the T -dependent constant

$$c(T) := \cos \frac{\pi}{T}.$$

Accordingly, for fixed $\omega \in \mathbb{R}$, the Fourier extension g_n of the function (1) will begin to converge once n exceeds $\frac{1}{2}r(T)\omega$ (recall that g_n involves $2n + 1$ degrees of freedom). In particular, we find that $r(T) \sim 2T$ for $T \approx 1$ and $r(T) \sim \pi$ as $T \rightarrow \infty$. Note that the resolution of the function $f(x) = \exp(i\omega\pi x)$ using classical Fourier series on $[-T, T]$ would require a minimum of $2T\omega$ degrees of freedom (whenever f is periodic). Thus, Fourier extensions exhibit comparable performance for T close to 1. However, as T increases, f can be resolved far more efficiently via its Fourier extension than if it had been directly expanded in a Fourier series on $[-T, T]$. In particular, the resolution power is bounded above for all T by π , which is precisely the resolution constant for polynomial approximations.

Aside from establishing when asymptotic convergence will occur, we also show that the convergence in this regime is exponential at rate $\rho^{-n} = E(T)^{-n}$, where

$$E(T) = \frac{3 + c(T) + 2\sqrt{2 + 2c(T)}}{1 - c(T)},$$

(this result actually holds for all sufficiently analytic functions f , not just (1)). Here, we note that $E(1) = 1$, implying no exponential convergence for $T = 1$. This is of course a consequence of the Gibbs phenomenon of Fourier series on $[-1, 1]$. Convergence is exponential for all T greater than 1, however, and the rate increases with increasing T .

Hence, the main conclusion we draw in this paper is the following. Smaller T yields better resolution power of Fourier extensions, at a cost of slower, but still exponential, convergence. Conversely, larger T yields faster exponential convergence, at the expense of reduced resolution power. Formally, one may also obtain a resolution constant of 2 in the limit $n \rightarrow \infty$ by allowing $T \rightarrow 1$ as $n \rightarrow \infty$, albeit with a deterioration of the convergence rate to subexponential.

This aside, we also present a new numerical method for computing Fourier extensions. Straightforward implementation of (3), known as the Galerkin method, is severely ill-conditioned. As a result, the best attainable accuracy with this approach is of order $\sqrt{\epsilon}$, where ϵ is the machine precision used. To counter this, we present a new collocation method, based on a judicious choice

of nodes (related to certain Gaussian quadratures), which leads to far less severe condition numbers. Numerical examples demonstrate much higher attainable accuracies with this approach, typically of order ϵ .

Unfortunately, any implementation of (3), be it Galerkin, collocation or otherwise, in a basis of complex exponentials is ill-conditioned. This means that the result of any numerical computation may differ somewhat from the exact solution of (3). We discuss this observation and its consequences in some detail.

The outline of the remainder of this paper is as follows. In §2 we detail the convergence of Fourier extensions for arbitrary $T > 1$ and discuss the numerical solution of Problem 1.1. In §3 we explore the resolution power of polynomial expansions, since similar techniques shall be used later. Finally, §4 is devoted to the question of resolution power of Fourier extensions.

2 Fourier extensions on arbitrary intervals

In this section, we first show that the solution to the Fourier extension problem converges spectrally for all smooth functions f and for all $T > 1$. Next, a more involved analysis in §2.2 demonstrates that the Fourier extension does converge exponentially whenever f is analytic. Finally, in §2.3 we discuss issues arising in the numerical computation of Fourier extensions, and introduce a new collocation scheme with improved performance.

2.1 Spectral convergence

Common spectral methods based on orthogonal polynomials (or Fourier series in the periodic case) converge exponentially fast provided f is analytic, and spectrally fast if f is only smooth in $[-1, 1]$ [11, chpts 2,5]. Whenever f has only finite regularity, convergence is algebraic at a rate determined by the degree of smoothness: specifically, if f is $(k-1)$ -times continuously differentiable and $f^{(k)}$ exists almost everywhere and is square-integrable (equivalently, $f \in H^k[-1, 1]$, the k th standard Sobolev space of functions defined on $[-1, 1]$), then f_n converges algebraically fast at rate k . Our first result regarding Fourier extensions illustrates identical convergence in this setting:

Theorem 2.1. *Suppose that $f \in H^k[-1, 1]$ for some $k \in \mathbb{N}$ and that $T_0 > 1$. Then, for all $n \in \mathbb{N}$ and $T \geq T_0$,*

$$\|f - g_n\|_{L^2_{[-1,1]}} \leq c_k(T_0) \left(\frac{n\pi}{T}\right)^{-k} \|f\|_{H^k_{[-1,1]}}, \quad (5)$$

where $c_k(T_0) > 0$ is independent of n , f and T , $\|\cdot\|_{H^k_{[-1,1]}}$ is the standard norm on $H^k[-1, 1]$ and g_n is the exact Fourier extension of f on $[-T, T]$ defined by (3).

Proof. Recall that there exists an extension operator $\mathcal{E} : H^k[-1, 1] \rightarrow H^k(\mathbb{R})$ with $\mathcal{E}f|_{[-1,1]} = f$ and $\|\mathcal{E}f\|_{H^k_{\mathbb{R}}} \leq c\|f\|_{H^k_{[-1,1]}}$ for some positive constant c independent of f [1].

Let $\chi \in C^\infty(\mathbb{R})$ be monotonically decreasing and satisfy $\chi(x) = 0$ for $x > T_0 - 1$ and $\chi(x) = 1$ for $x < 0$. We define the bump function $\mathcal{B} \in C^\infty(\mathbb{R})$ by

$$\mathcal{B}(x) = \begin{cases} \chi(-x-1) & -T_0 \leq x < -1 \\ 1 & -1 \leq x \leq 1 \\ \chi(x-1) & 1 < x \leq T_0 \\ 0 & |x| > T_0. \end{cases}$$

Note that the function $\mathcal{B}(x)\mathcal{E}f(x) \in H^k(\mathbb{R})$ has support in $[-T_0, T_0]$ and thus its restriction to $[-T, T]$ is periodic for any $T \geq T_0$. Since g_n minimises the L^2 norm error over all functions from the set G_n , we have

$$\|f - g_n\|_{L^2_{[-1,1]}} \leq \|f - (\mathcal{B}\mathcal{E}f)_n\|_{L^2_{[-1,1]}} \leq \|\mathcal{B}\mathcal{E}f - (\mathcal{B}\mathcal{E}f)_n\|_{L^2_{[-T,T]}}$$

where $(\mathcal{B}\mathcal{E}f)_n$ is the n th partial Fourier sum of $\mathcal{B}(x)\mathcal{E}f(x)$ on $[-T, T]$. Since $\mathcal{B}\mathcal{E}f \in H^k[-T, T]$ and is periodic on $[-T, T]$, a well-known estimate [11, eqn (5.1.10)] gives

$$\|\mathcal{B}\mathcal{E}f - (\mathcal{B}\mathcal{E}f)_n\|_{L^2_{[-T,T]}} \leq \left(\frac{n\pi}{T}\right)^{-k} \|(\mathcal{B}\mathcal{E}f)^{(k)}\|_{L^2_{[-T,T]}}.$$

Since $\|(\mathcal{B}\mathcal{E}f)^{(k)}\|_{L^2_{[-T,T]}} = \|(\mathcal{B}\mathcal{E}f)^{(k)}\|_{L^2_{[-T_0, T_0]}} \leq c_k(T_0)\|f\|_{H^k_{[-1,1]}}$ for some constant $c_k(T_0)$ independent of f , the result now follows immediately. \square

2.2 Exponential convergence

2.2.1 The exact solution

As mentioned in the introduction, the exact solution of Problem 1.1 can be characterized in terms of certain nonclassical orthogonal polynomial expansions. This was demonstrated for the case $T = 2$ in [19], but can be shown for any $T > 1$ with relatively minor modifications.

Our approach is to construct an orthogonal basis for the space G_n of $2T$ -periodic functions. Since the least squares criterion in the Fourier extension problem corresponds to an orthogonal projection, it then suffices to expand a given function f in this basis in order to find its Fourier extension.

The cosines and sines are already mutually orthogonal and can be treated separately. Consider the cosines first, i.e., we have the set

$$C_n := \left\{ \cos \frac{\pi}{T} kx \right\}_{k=0}^n.$$

Trigonometric functions are closely related to polynomials, through an appropriate *cosine-mapping*. This can be seen, for example, from the defining property of Chebyshev polynomials of the first kind T_k ,

$$\cos kx = T_k(\cos x).$$

In the same spirit, we define the map

$$y = \cos \frac{\pi}{T} x, \tag{6}$$

and note that if $\cos kx$ is a polynomial in $\cos x$, then $\cos \frac{\pi}{T} kx$ is a polynomial in y . It follows that the cosines in C_n are exactly polynomials in y up to degree n .

Since the functions in C_n are linearly independent, an orthogonal basis exists. Moreover, without loss of generality, we may write the basis functions as polynomials in y , say $T_k^T(y) = T_k^T(\cos \frac{\pi}{T}x)$. Orthogonality in $L^2_{[-1,1]}$ implies

$$\begin{aligned}\delta_{k-l} &= \int_{-1}^1 T_k^T(\cos \frac{\pi}{T}x) T_l^T(\cos \frac{\pi}{T}x) dx \\ &= 2 \int_0^1 T_k^T(\cos \frac{\pi}{T}x) T_l^T(\cos \frac{\pi}{T}x) dx \\ &= \frac{2T}{\pi} \int_{c(T)}^1 T_k^T(y) T_l^T(y) \frac{1}{\sqrt{1-y^2}} dy.\end{aligned}$$

In the latter step, we applied the substitution (6), which maps the interval $[0, 1]$ to $[c(T), 1]$ (recall that $c(T) = \cos \frac{\pi}{T}$) and introduces the Jacobian with the inverse square root. It follows that the $T_k^T(y)$ are orthonormal polynomials with respect to the weight function

$$w_1(y) = \frac{2T}{\pi} \frac{1}{\sqrt{1-y^2}}.$$

This weight differs only by a constant factor from the typical weight function of Chebyshev polynomials of the first kind $T_k(y)$. However, the interval of orthogonality is different from that of the Chebyshev polynomials, since $[c(T), 1]$ is contained within $(-1, 1]$ for $T > 1$, and Chebyshev polynomials are orthogonal over the whole interval $[-1, 1]$.

We now consider the set of sines in G_n ,

$$S_n := \{\sin \frac{\pi}{T}kx\}_{k=1}^n.$$

They lead to orthogonal polynomials resembling Chebyshev polynomials of the second kind $U_k(y)$ in the following way. From the property

$$\sin(k+1)x = U_k(\cos x) \sin x$$

we find that $\sin \frac{\pi}{T}kx$ is also a polynomial in y , but only up to an additional factor. This factor is

$$\sin \frac{\pi}{T}x = \sqrt{1-y^2}.$$

We therefore consider an orthogonal basis in the form

$$U_k^T(y) \sqrt{1-y^2} = U_k^T(\cos \frac{\pi}{T}x) \sin \frac{\pi}{T}x.$$

Orthogonality in $L^2_{[-1,1]}$ implies

$$\begin{aligned}\delta_{k-l} &= \int_{-1}^1 U_k^T(\cos \frac{\pi}{T}x) \sin \frac{\pi}{T}x U_l^T(\cos \frac{\pi}{T}x) \sin \frac{\pi}{T}x dx \\ &= 2 \int_0^1 U_k^T(\cos \frac{\pi}{T}x) \sin \frac{\pi}{T}x U_l^T(\cos \frac{\pi}{T}x) \sin \frac{\pi}{T}x dx \\ &= \frac{2T}{\pi} \int_{c(T)}^1 U_k^T(y) U_l^T(y) \sqrt{1-y^2} dy.\end{aligned}$$

Thus, the $U_k^T(y)$ are again orthonormal polynomials. The weight function

$$w_2(y) = \frac{2T}{\pi} \sqrt{1 - y^2}$$

corresponds to that of the Chebyshev polynomials of the second kind, but here too the interval of orthogonality differs from the classical case in the same T -dependent manner.

Note that we have essentially proved the following theorem.

Theorem 2.2. *The solution to Problem 1.1 is*

$$g_n(x) = \sum_{k=0}^n a_k T_k^T \left(\cos \frac{\pi}{T} x \right) + \sum_{k=0}^{n-1} b_k U_k^T \left(\cos \frac{\pi}{T} x \right) \sin \frac{\pi}{T} x,$$

with

$$a_k = \int_{-1}^1 f(x) T_k^T \left(\cos \frac{\pi}{T} x \right) dx, \quad (7)$$

$$b_k = \int_{-1}^1 f(x) U_k^T \left(\cos \frac{\pi}{T} x \right) \sin \frac{\pi}{T} x dx, \quad (8)$$

and where the polynomials $T_k^T(y)$ and $U_k^T(y)$ orthonormal on $[c(T), 1]$ with respect to the weights $w_1(y)$ and $w_2(y)$ defined above.

Proof. The result follows directly from the facts that g_n is the orthogonal projection of f onto the space G_n and the functions $T_k^T(\cos \frac{\pi}{T} x)$, $U_k^T(\cos \frac{\pi}{T} x) \sin \frac{\pi}{T} x$ comprise an orthogonal basis for this space. \square

2.2.2 Expansions in orthogonal polynomials

Since Fourier extensions are related to expansions in orthogonal polynomials, we briefly recall important properties of such expansions that we will use further on. For an in-depth treatment of this topic, we refer the reader to [4, 24, 25].

The convergence rate of the expansion of a function f in a set of orthogonal polynomials is exponential when f is analytic. For a wide class of orthogonal polynomials on the interval $[-1, 1]$, the precise rate of convergence is determined by the largest *Bernstein ellipse* within which f is analytic. A Bernstein ellipse is given by

$$e(\rho) := \left\{ \frac{1}{2}(\rho^{-1} e^{-i\theta} + \rho e^{i\theta}) : \theta \in [-\pi, \pi] \right\}.$$

Since $e(\rho)$ and $e(1/\rho)$ are the same we restrict the definition to $\rho \geq 1$. Note that ρ is the sum of the major and minor semiaxis lengths of the ellipse and the ellipse has foci ± 1 . The convergence rate of the expansion of a function f , analytic in $e(\rho)$, in a set of orthogonal polynomials on $[-1, 1]$ is precisely ρ^{-n} .

Singularities of f in the complex plane limit the possible sizes of the Bernstein ellipses in which f is analytic. In particular, they limit the range of ρ . The *closest singularity* of f is the one that imposes the most stringent limit on ρ and it determines the convergence rate $\rho = \rho_{\max}$.

2.2.3 Exponential convergence of the exact solution

The functions being expanded in the theory of the Fourier extension problem above are related to f through the inverse of the map (6). We will have to distinguish between the even and odd parts of f ,

$$\begin{aligned} f_e(x) &= \frac{f(x) + f(-x)}{2}, \\ f_o(x) &= \frac{f(x) - f(-x)}{2}. \end{aligned}$$

From

$$\begin{aligned} a_k &= \int_{-1}^1 f(x) T_k^T(\cos \frac{\pi}{T} x) dx \\ &= 2 \int_0^1 f_e(x) T_k^T(\cos \frac{\pi}{T} x) dx \\ &= \frac{2T}{\pi} \int_{c(T)}^1 f_e\left(\frac{T}{\pi} \cos^{-1} y\right) T_k^T(y) \frac{1}{\sqrt{1-y^2}} dy, \end{aligned} \quad (9)$$

we see that the even part of the Fourier extension g_n is precisely the orthogonal polynomial expansion of the function

$$f_1(y) = f_e\left(\frac{T}{\pi} \cos^{-1} y\right) = f_e(x).$$

A similar reasoning for the odd part of f , based on the coefficients b_k , yields the second function

$$f_2(y) = \frac{f_o\left(\frac{T}{\pi} \cos^{-1} y\right)}{\sqrt{1-y^2}} = \frac{f_o(x)}{\sin \frac{\pi}{T} x},$$

with the odd part of g_n , when divided by $\sin \frac{\pi}{T} x$, corresponding to the expansion of f_2 in the polynomials $U_k^T(y)$.

The convergence rate of the Fourier extension problem will be determined by the nearest singularity of $f_1(y)$ or $f_2(y)$ to the interval $[c(T), 1]$. Note that, even when f is analytic in a very large region, singularities are introduced by the inverse cosine at the points $y = -1$ and $y = 1$. One can verify that the singularity at $y = 1$ is removable both for f_1 and f_2 . Thus, the nearest singularity lies at $y = -1$.

In order to apply the theory outlined in §2.2.2, it remains to map the interval $[c(T), 1]$ to the standard interval $[-1, 1]$. This is achieved by the affine map

$$m^{-1}(s) = 2 \frac{s - c(T)}{1 - c(T)} - 1, \quad s \in [c(T), 1], \quad (10)$$

with inverse $m(t) = \frac{1}{2}(1 - c(T))s + \frac{1}{2}(1 + c(T))$ mapping $[-1, 1]$ to $[c(T), 1]$. Note that m^{-1} maps the point $y = -1$ to the point

$$u = \frac{3 + c(T)}{c(T) - 1}.$$

This point lies on the negative real axis. The Bernstein ellipse $e(\rho)$ crosses the negative real axis in the point $-\frac{1}{2}(\rho^{-1} + \rho)$. Equating this with u yields the maximal ρ .

We therefore deduce the following result:

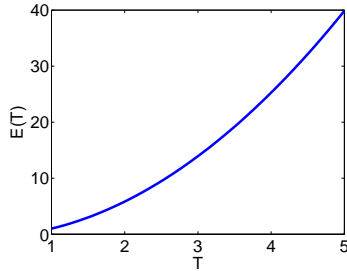


Figure 1: Theoretical convergence rate of Fourier extensions as a function of the extension parameter T .

Theorem 2.3. *For sufficiently analytic f , the error in the approximation of f by its Fourier extension g_n behaves as*

$$|f(x) - g_n(x)| \sim E(T)^{-n}, \quad n \rightarrow \infty, \quad -1 \leq x \leq 1,$$

with

$$E(T) = \frac{3 + c(T) + 2\sqrt{2 + 2c(T)}}{1 - c(T)}.$$

This theorem generalizes Theorem 3.14 of [19] to the case of general $T > 1$. For the sake of brevity, we have limited the exposition here to the case of a sufficiently analytic function f . Yet, we make the following comments:

- The convergence rate may be slower than $E(T)^{-n}$ when $f(x)$ is not sufficiently analytic as a function of x , i.e., if f has a singularity closer than that introduced by the inverse cosine mapping.
- The convergence may also be faster than $E(T)^{-n}$, if f is analytic and periodic on $[-T, T]$. In that case, one can verify that the singularity introduced by the inverse cosine at $y = -1$ is also removable. Thus, the convergence rate is no longer limited by the singularity of the map between x and y .
- For the case $T = 2$ we recover the convergence rate $E(2) = 3 + 2\sqrt{2}$ found in [19, §3.4].

The function $E(T)$ is depicted in Fig. 1. It is monotonically increasing on $(1, \infty)$ as a function of T . It behaves as $1 + \pi(T - 1)$ for $T \approx 1$ and as $\frac{16}{\pi^2}T^2$ for $T \gg 1$. Thus, larger T leads to more rapid exponential convergence. This is confirmed in Fig. 2, where we plot the error in approximating $f(x) = e^x$ by f_n for various n and T (for this example we use high precision to avoid any numerical effects). Note the close correspondence between the observed and predicted convergence rates, as well as the significant increase in convergence rate for larger T . Having said this, it turns out that increasing T also adversely affects the stability of numerical computation of the Fourier extension, a topic we consider in the next section.

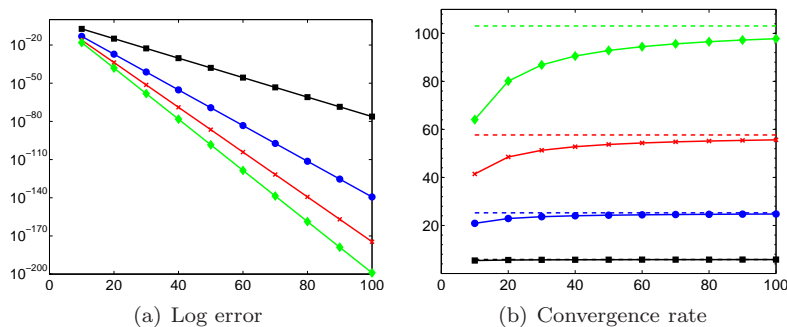


Figure 2: The quantities $e_n = \|f - g_n\|_{L^\infty[-1,1]}$ (solid line) and $E(T)^{-n}$ (dashed line) for $T = 2, 4, 6, 8$. The left panel shows the values e_n and $E(T)^{-n}$. The right panel gives the scaled values $\exp(-\frac{1}{n} \log e_n)$ and $E(T)$.

2.3 Numerical solution

Most straightforward numerical implementations of Problem 1.1 (the Fourier extension problem) suffer from severe ill-conditioning. The reason is simple: although the functions $\cos \frac{\pi}{T} kx$ and $\sin \frac{\pi}{T} kx$ form an orthogonal basis on $[-T, T]$, they only constitute a frame when restricted to the interval $[-1, 1]$. In fact,

Lemma 2.4. *The set*

$$\Phi := \left\{ \frac{1}{\sqrt{2}} \right\} \cup \left\{ \frac{1}{\sqrt{2}} \exp(i \frac{k\pi}{T} x) \right\}_{k \in \mathbb{Z} \setminus \{0\}}, \quad (11)$$

is a normalized tight frame for $L^2[-1, 1]$ with frame bound T .

Proof. Let $f \in L^2[-1, 1]$ be given and define $\tilde{f} \in L^2[-T, T]$ as the extension of f to $[-T, T]$ by zero. Since

$$a_k = \frac{1}{\sqrt{2}} \int_{-1}^1 f(x) \exp(i \frac{k\pi}{T} x) dx = \frac{1}{\sqrt{2}} \int_{-T}^T \tilde{f}(x) \exp(i \frac{k\pi}{T} x) dx, \quad (12)$$

we find that $\frac{1}{\sqrt{T}} a_k$ is precisely the k th Fourier coefficient of \tilde{f} on $[-T, T]$. By Parseval's relation

$$\sum_{k=-\infty}^{\infty} |a_k|^2 = T \|\tilde{f}\|^2 = T \|f\|^2,$$

as required. \square

For a general introduction to the theory of frames, see [12].

Lemma 2.4 has several implications, since a given function f may have many representations in a frame, and such representations may have strongly contrasting properties. For example, associated to any frame $\{f_k\}$ is the so-called canonical dual frame $\{g_k\}$ [12]. A representation of f , the *frame decomposition*, is given in terms of this frame by

$$f = \sum_{k=1}^{\infty} \langle f, g_k \rangle f_k.$$

Since the frame (11) is tight, it coincides with its canonical dual up to a constant factor that is equal to the frame bound, in this case T . Therefore its frame decomposition is precisely

$$\sum_{k=-\infty}^{\infty} \frac{1}{\sqrt{T}} a_k \frac{\exp(i \frac{k\pi}{T} x)}{\sqrt{2T}},$$

where the a_k 's are given by (12). However, as illustrated in the proof of the previous lemma, this is precisely the Fourier series of the discontinuous function \tilde{f} , and thus this infinite series converges only slowly and suffers from a Gibbs phenomenon. On the other hand, as shown in the proof of Theorem 2.1, by extending f smoothly to $[-T, T]$, one can obtain representations of f that converge spectrally fast.

Clearly, given its exponential rate of convergence, the exact Fourier extension g_n need not coincide with any of the aforementioned representations. Moreover, it is not certain that the result of any numerical implementation will coincide with g_n . This has a significant potential consequence: theoretical estimates for the exact solution are not guaranteed to be carried over to any numerical solution.

2.3.1 The Galerkin method

The most straightforward numerical implementation of the Fourier extension method involves computing the solution g_n to (3) exactly. Letting $\{\phi_j\}_{j=1}^{2n+1}$ be a basis for the set G_n , this is equivalent to solving the linear system $Ax = B$, where $A \in \mathbb{R}^{(2n+1) \times (2n+1)}$ and $B \in \mathbb{R}^{2n+1}$ have entries $\langle \phi_k, \phi_j \rangle$ and $\langle f, \phi_j \rangle$ respectively. The drawbacks of this approach are twofold. First, it requires knowledge (or prior computation) of the integrals $\langle f, \phi_j \rangle$. Second, it results in a condition number $\kappa(A) \sim E(T)^{2n}$. Such severe ill-conditioning typically limits the accuracy of this numerical implementation to only $\mathcal{O}(\sqrt{\epsilon})$, where ϵ is the machine precision used [19].

2.3.2 A collocation method

It transpires that both these issues can be resolved by replacing this Galerkin approach with one defined by collocation based on a judicious choice of nodes. Thus, if $\{x_i\}_{i=1}^{2n+1} \in [-1, 1]$ we instead define \tilde{A} and \tilde{B} by $\phi_k(x_j)$ and $f(x_j)$ respectively, and solve $\tilde{A}x = \tilde{B}$.

The key question is how to determine good collocation nodes. Recall that g_n , as defined by (3), is essentially a sum of two polynomial approximations in the variable $y \in [c(T), 1]$. The polynomial interpolant of an analytic function in y at Chebyshev nodes (appropriately scaled to the interval $[c(T), 1]$) converges exponentially fast at the same rate ρ . Therefore, such nodes, when mapped to the original domain via $x = \frac{T}{\pi} \cos^{-1} y$, will ensure exponential convergence of the resultant Fourier extension at rate $E(T)$.

It is now slightly easier to redefine G_n to be the space of dimension $2n + 2$ spanned by the functions $\{\cos \frac{\pi}{T} kx\}_{k=0}^n$ and $\{\sin \frac{\pi}{T} kx\}_{k=1}^{n+1}$. The $2n + 2$ collocation nodes in $[-1, 1]$ therefore take the form $\{x_i\}_{i=0}^n \cup \{-x_i\}_{i=0}^n$, where

$$x_i = \frac{T}{\pi} \cos^{-1} \left[\frac{1}{2}(1 - c(T)) \cos \left(\frac{(2i+1)\pi}{2n+2} \right) + \frac{1}{2}(1 + c(T)) \right], \quad i = 0, \dots, n.$$

Recall that $c(T) = \cos \frac{\pi}{T}$. We refer to such nodes as *symmetric mapped Chebyshev nodes*.

Let us illustrate how this choice of nodes improves conditioning. We have

Lemma 2.5. *Let \tilde{A} be the collocation matrix based on the symmetric mapped Chebyshev nodes, and suppose that D is the diagonal matrix of weights $\omega_i = \frac{\pi}{n+1}$. Then $A = \tilde{A}^\top D \tilde{A}$ has entries*

$$\langle \phi_k, \phi_j \rangle_W = \int_{-1}^1 \phi_j(x) \phi_k(x) W(x) dx, \quad j, k = 1, \dots, 2n+2,$$

where W is a positive, integrable function given by

$$W(x) = \frac{2\pi}{T} \frac{\cos \frac{\pi}{2T} x}{\sqrt{2 \cos \frac{\pi}{T} x - 1}}.$$

In particular, A is precisely the Galerkin matrix of the Fourier extension problem defined in the weighted space $L_W^2[-1, 1]$ of square integrable functions with respect to $W(x)$.

Proof. Note that A is a block matrix with nonzero blocks corresponding to inner products of cosines with cosines and sines with sines. Consider first the block of A corresponding to the cosine functions $\cos \frac{\pi}{T} kx$. In the (j, k) th entry, using the symmetry of the collocation points, we have that

$$2 \sum_{i=0}^n \omega_i \phi_j(x_i) \phi_k(x_i) = 2 \sum_{i=0}^n \omega_i T_j(y_i) T_k(y_i),$$

where $\{y_i\}_{i=0}^n = \cos(\frac{\pi}{T} x_i)$ are Chebyshev nodes on $[c(T), 1]$. Recall that $m(t)$ is a map from $[-1, 1]$ to $[c(T), 1]$, as defined in §2.2.3. Since the product $T_j(y) T_k(y)$ is a polynomial in y of degree at most $2n$, the Gaussian quadrature rule associated with the points x_i is exact and it follows that

$$\begin{aligned} 2 \sum_{i=0}^n \omega_i \phi_j(x_i) \phi_k(x_i) &= 2 \int_{-1}^1 T_j(m(t)) T_k(m(t)) \frac{1}{\sqrt{1-t^2}} dt \\ &= 2 \int_{c(T)}^1 T_j(y) T_k(y) w(y) dy, \end{aligned}$$

where $w(y)$ is given by

$$w(y) = \frac{2}{1-c(T)} \frac{1}{\sqrt{1 - \left(\frac{2y-1-c(T)}{1-c(T)} \right)^2}}.$$

The first factor is the Jacobian of the mapping to $[c(T), 1]$, the second factor is the scaling of the standard Chebyshev weight to that interval. The change of variables $y = \cos \frac{\pi}{T} x$ now gives

$$2 \sum_{i=0}^n \omega_i \phi_j(x_i) \phi_k(x_i) = 2 \frac{\pi}{T} \int_0^1 \phi_j(x) \phi_k(x) w(\cos \frac{\pi}{T} x) \sin \frac{\pi}{T} x dx,$$

which is easily found to coincide with $\langle \phi_k, \phi_j \rangle_W$. The case corresponding to the sine functions $\sin \frac{\pi}{T} kx$ is identical. \square

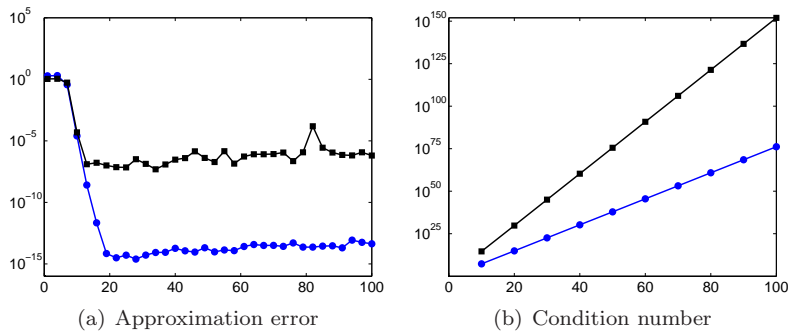


Figure 3: The approximation errors $\|f - g_n\|_{L^\infty[-1,1]}$ (left panel) and condition numbers $\kappa(A)$ (right panel) for the Galerkin (squares) and collocation (circles) methods with $T = 2$ and $f(x) = \cos 16x$.

This lemma indicates that $\kappa(\tilde{A}) \approx (\kappa(A))^{\frac{1}{2}}$. Since A is the matrix of a Galerkin method and W is an integrable weight function, we may expect that $\kappa(A) \approx E(T)^{2n}$, i.e. exactly as in the unweighted case. Therefore, collocation leads to the significant reduction in condition number, with $\kappa(\tilde{A}) \approx E(T)^n$ as opposed to $E(T)^{2n}$. As a result, one typically observes a much higher accuracy, $\mathcal{O}(\epsilon)$ as opposed to $\mathcal{O}(\sqrt{\epsilon})$, with this approach.

This improvement is illustrated in Fig. 3 for the example $f(x) = \cos 16x$. As shown in the left panel, the best attainable error with the Galerkin approach is roughly 10^{-8} , whereas the collocation method obtains much closer to machine epsilon. The right panel indicates the significantly milder growth in condition number.

Such an improvement is by no means unique to this choice of nodes. A suitable alternative choice of collocation points follows from using the roots of the polynomials $T_k^T(y)$. With an appropriate number of points, the matrix $\tilde{A}^T D \tilde{A}$, with D containing the weights of the associated Gaussian quadrature rule on its diagonal, is precisely the Galerkin discretization of the unweighted least squares problem, rather than the weighted problem that was identified in Lemma 2.5. The use of these points as Gaussian quadrature was already explored in [19]. However, these points depend on T in a non-trivial way and, although they can easily be computed, are not available in closed form. As numerical experiments indicate that the performance of such point sets is not significantly better than the points proposed in this section, we forego a more detailed analysis.

3 Resolution power of polynomial expansions

Having introduced and analysed Fourier extensions, and discussed their numerical implementation, in the next section we establish their resolution power. Before doing so, since similar techniques will be used subsequently, we first derive the well-known result for orthogonal polynomial expansions.

Suppose that $f(x)$ is given on $[-1, 1]$ and is analytic in a neighbourhood thereof. Let $f_n \in \mathbb{P}_n$ be its n -term expansion in orthogonal polynomials with

respect to the positive and integrable weight function $w(x)$. If $L_w^2[-1, 1]$ is the space of weighted square integrable functions with respect to w , then f_n is given by

$$f_n := \arg \min_{p \in \mathbb{P}_n} \|f - p\|_{L_{[-1,1],w}^2}.$$

In particular, for any $p_n \in \mathcal{P}_n$,

$$\|f - f_n\|_{L_{[-1,1],w}^2}^2 \leq \|f - p_n\|_{L_{[-1,1],w}^2}^2 \leq \|w\|_{L_{[-1,1]}^1} \|f - p_n\|_{L_{[-1,1]}^\infty}^2.$$

Hence, to study of the resolution power of any orthogonal polynomial expansion it suffices to consider only one particular example. Without loss of generality, we now focus on expansions in Chebyshev polynomials (i.e. $w(x) = (1-x^2)^{-\frac{1}{2}}$), in which case

$$p_n(x) = \sum_{k=0}^n {}' a_k T_k(x), \quad f(x) = \sum_{k=0}^{\infty} {}' a_k T_k(x), \quad (13)$$

where

$$a_k = \int_0^\pi f(\cos \theta) \cos k\theta \, d\theta, \quad (14)$$

and $'$ indicates that the first term of the sum should be halved. Since the infinite sum (13) converges uniformly, we have the estimate

$$\|f - p_n\|_{L_{[-1,1]}^\infty} \leq \sum_{k>n} |a_k|.$$

Therefore, to study resolution power, it suffices to examine the nature of the coefficients a_n for the function

$$f(x) = \exp(i\pi\omega x). \quad (15)$$

To this end, we use the following standard estimate, given in [24, p.175]:

$$|a_n| \leq \frac{2M}{\rho^n}. \quad (16)$$

Here ρ corresponds to any Bernstein ellipse $e(\rho)$ in which f is analytic and M is the maximum of $|f(z)|$ along that ellipse.

For a given ω and n , we consider the minimum of all bounds of the form (16). Let us denote by M_ρ the maximum of f along $e(\rho)$. Since f is a complex exponential, f reaches a maximum at the point on the ellipse with the smallest (negative) imaginary part. This corresponds to $\theta = -\pi/2$ and we have

$$M_\rho = \exp\left(\pi\omega \frac{\rho^2 - 1}{2\rho}\right). \quad (17)$$

The bound (16) becomes

$$B(\omega, n, \rho) := \frac{2M_\rho}{\rho^n} = \frac{2 \exp\left(\pi\omega \frac{\rho^2 - 1}{2\rho}\right)}{\rho^n}. \quad (18)$$

For fixed ω and n , we find the minimal value of this bound by differentiating (18) with respect to ρ . Equating the derivative to zero

$$\frac{d}{d\rho}B(\omega, n, \rho) = 0, \quad (19)$$

yields two solutions

$$\frac{n \pm \sqrt{n^2 - \pi^2\omega^2}}{\pi\omega}. \quad (20)$$

Consider first the case $n < \pi\omega$. Both solutions of (19) are complex-valued. Note that

$$B(\omega, n, 1) = 2$$

and

$$\frac{d}{d\rho}B(\omega, n, 1) = 2\pi\omega - 2n.$$

It follows that B is strictly increasing as a function of ρ . For $n < \pi\omega$, the best possible bound for a_n of the form (16) is 2.

Consider next the case $n > \pi\omega$. Since it is easily seen that the roots (20) are inverses of each other, we restrict our attention to the one greater than 1, i.e.,

$$\rho_{min} := \frac{n + \sqrt{n^2 - \pi^2\omega^2}}{\pi\omega}.$$

Since $B(\omega, n, \rho)$ initially decays at $\rho = 1$, ρ_{min} is the unique minimum of the bound for $\rho > 1$. Thus,

$$B(\omega, n, \rho_{min}) < B(\omega, n, \rho), \quad \rho \in [1, \infty).$$

In particular, this implies exponential decay of the next coefficients:

$$|a_{n+k}| \leq B(\omega, n, \rho_{min}) \frac{1}{\rho_{min}^k} < \frac{2}{\rho_{min}^k}.$$

Finally, consider the value $n = \pi\omega$. Then $\rho = 1$ is a global minimum of the bound (18), since

$$\frac{d}{d\rho}B(\omega, \pi\omega, 1) = \frac{d^2}{d\rho^2}B(\omega, \pi\omega, 1) = 0,$$

and

$$\frac{d^3}{d\rho^3}B(\omega, \pi\omega, 1) = 2\pi\omega > 0.$$

In conclusion, we have seen that for an oscillatory function of the form (15), we need $n = \pi\omega$ degrees of freedom before exponential decay kicks in. This is π degrees of freedom per wavelength – the well-known resolution power of polynomials.

Note that this figure was previously derived in [15] for orthogonal polynomial expansions corresponding to the Gegenbauer weight $w(x) = (1 - x^2)^{\lambda - \frac{1}{2}}$, $\lambda > -\frac{1}{2}$ (see also [14, p.35] for $\lambda = 0$). This result was based on explicit expressions for the Gegenbauer polynomial expansion of e^{ixt} . The previous arguments generalize this result to arbitrary weight functions $w(x)$.

4 Resolution power of Fourier extensions

We now consider the resolution power of Fourier extensions. To this end, we divide our attention between the exact Fourier extension, i.e. g_n as defined by (3), and that obtained from the numerical implementation introduced in §2.3. We commence with the former.

4.1 Resolution power of the exact solution

A naïve estimate for the resolution constant $r(T)$ follows immediately from the bound (5) in Theorem 2.1. Indeed, for $f(x) = \exp(i\omega\pi x)$ we have

$$\|f\|_{H^k_{[-1,1]}} = \mathcal{O}(\omega\pi)^k, \quad k = 1, 2, \dots,$$

and therefore $r(T)$ satisfies $r(T) \leq 2T$, with spectral convergence occurring once n exceeds ωT . On first viewing, this estimate seems plausible. For example, consider the special situation where the frequency of oscillation ω is an integer multiple of T^{-1} . Then the function $f(x) = \exp(i\frac{\pi}{T}mx)$ is precisely the m th complex exponential in the Fourier basis on $[-T, T]$. Given that the Fourier extension g_n of f is error minimising amongst all functions in G_n , we can expect f to be recovered exactly by its Fourier extension whenever $n \geq m = \omega T$. Thus, for oscillations at frequencies $\omega = \frac{m}{T}$, $m \in \mathbb{Z}$, the estimate $r(T) \leq 2T$ appears correct. However, numerical results (see §4.4) indicate that such an estimate is only accurate for small T : for large T it transpires that $r(T) \sim \pi$, a result we shall prove subsequently. Before doing so, however, let us note the following unexpected conclusion: for large T , we can resolve the oscillatory exponentials $\exp(i\frac{\pi}{T}mx)$ accurately on $[-1, 1]$ using Fourier extensions comprised of relatively non-oscillatory exponentials $\exp(i\frac{\pi}{T}nx)$, $n \ll m$.

To obtain an accurate estimate for $r(T)$, we need to argue along the same lines as §2.2 and exploit the close relationship between Fourier extensions and certain orthogonal polynomial expansions. Recall that the theory of §2.2 treats even and odd cases separately. Let us first assume that f is even, so that

$$f(x) = \cos \omega\pi x$$

(we consider the odd case later). Upon applying the transformation $x = \frac{T}{\pi} \cos^{-1} y$ we obtain

$$f_1(y) = \cos \omega T \cos^{-1} y, \quad y \in [c(T), 1].$$

The Fourier extension of $f(x)$ is precisely the expansion of $f_1(y)$ in the orthogonal polynomials $T_k^T(y)$. If we now map the domain $[c(T), 1]$ to $[-1, 1]$ via

$$u = \frac{c(T) + 1 - 2y}{c(T) - 1}, \quad y = \frac{u}{2}(1 - c(T)) + \frac{1}{2}(1 + c(T)),$$

then this equates to an orthogonal polynomial expansion of the function

$$f_2(u) = \cos \left[\omega T \cos^{-1} \left(\frac{u}{2}(1 - c(T)) + \frac{1}{2}(1 + c(T)) \right) \right], \quad u \in [-1, 1]. \quad (21)$$

Thus, as in §3, to determine the resolution power of g_n , it suffices to consider the expansion of $f_2(u)$ in Chebyshev polynomials on $[-1, 1]$.

In view of the bound (16), we now seek the maximum value of $f_2(u)$ along the Bernstein ellipse $e(\rho)$. We first require

Lemma 4.1. For $\rho < E(T)$ and sufficiently large ω , the maximum value of $|f_2(u)|$ on the Bernstein ellipse $e(\rho)$ occurs at $\theta = 0$.

Proof. Let $z = x + iy$. Then

$$|\cos \omega z|^2 = \frac{1}{2} (\cos 2\omega x + \cosh 2\omega y).$$

Hence, for sufficiently large ω , the maximal value of $|\cos \omega z|$ on some curve C in the complex plane occurs at the point $z \in C$ where $|\Im z|$ is maximized.

When $u = \frac{1}{2}(\rho^{-1}e^{-i\theta} + \rho e^{i\theta})$, we may write $f_2(u) = \cos \omega T[X(\theta) + iY(\theta)]$, where $X(\theta)$ and $Y(\theta)$ are defined by

$$\cos [X(\theta) + iY(\theta)] = \frac{u}{2}(1 - c(T)) + \frac{1}{2}(1 + c(T)) = A(\theta) + iB(\theta),$$

and

$$A(\theta) = \frac{1}{2}(1 - c(T)) \cosh \rho \cos \theta + \frac{1}{2}(1 + c(T)), \quad B(\theta) = \frac{1}{2}(1 - c(T)) \sinh \rho \sin \theta.$$

Expanding the cosine, and equating real and imaginary parts, we find that

$$\cos X(\theta) \cosh Y(\theta) = A(\theta), \quad \sin X(\theta) \sinh Y(\theta) = B(\theta).$$

We seek to maximize $|Y(\theta)|$. Note trivially that $Y(\theta)$ cannot vanish identically for all θ , and thus it suffices to consider only those θ for which $Y(\theta) > 0$. Let $Z(\theta) = \cosh^2 Y(\theta)$. Then $Z(\theta)$ is defined by

$$\frac{A^2(\theta)}{Z(\theta)} + \frac{B^2(\theta)}{Z(\theta) - 1} = 1.$$

Rearranging,

$$Z^2(\theta) - (1 + A^2(\theta) + B^2(\theta))Z(\theta) + A^2(\theta) = 0.$$

To complete the proof, it suffices to show that Z attains its maximum value at $\theta = 0$. Suppose not. Then $Z'(\theta_0) = 0$ for some $\theta_0 \neq 0$ (with $Z(\theta_0) > 1$), and, after differentiating the above expression and rearranging, we obtain

$$\begin{aligned} Z(\theta_0) &= \frac{A'(\theta_0)A(\theta_0)}{A'(\theta_0)A(\theta_0) + B'(\theta_0)B(\theta_0)} \\ &= \frac{\cosh \rho [1 + c(T) - (c(T) - 1) \cosh \rho \cos \theta_0]}{(1 - c(T)) \cos \theta_0 + (1 + c(T)) \cosh \rho}. \end{aligned} \quad (22)$$

This expression is only valid if the denominator does not vanish. Suppose for the moment that it does, so that

$$\cos \theta_0 = \frac{1 + c(T)}{c(T) - 1} \cosh \rho.$$

In this case, we must also have that the numerator $A'(\theta)A(\theta) = 0$. However, this is equivalent to

$$\cos \theta_0 = \frac{1 + c(T)}{c(T) - 1} \operatorname{sech} \rho,$$

which contradicts the previous expression for $\cos \theta_0$ (recall that $\rho > 1$). Hence, the expression (22) is valid. With this to hand, we now substitute (22) into the quadratic equation for $Z(\theta)$ to give

$$(\cos \theta_0 - \cosh \rho)^2 ((c(T) - 1) \cosh \rho \cos \theta_0 - (1 + c(T))) = 0.$$

Since $\rho > 1$, we must have that

$$\cos \theta_0 = \frac{1 + c(T)}{(c(T) - 1)} \operatorname{sech} \rho.$$

However, substituting this into (22), gives $Z(\theta_0) = 0$, a contradiction (recall that $Z(\theta) > 1$). \square

Using this lemma, we deduce that the n th coefficient a_n of the Chebyshev expansion of $f_2(u)$ is bounded by

$$\begin{aligned} B(\omega, n, \rho, T) &= \frac{2}{\rho^n} \cos \left[\omega T \cos^{-1} \left(\frac{1}{4} \left(\rho + \frac{1}{\rho} \right) (1 - c(T)) + \frac{1}{2} (1 + c(T)) \right) \right] \\ &= \frac{2}{\rho^n} \cos \left[i\omega T \cosh^{-1} \left(\frac{1}{4} \left(\rho + \frac{1}{\rho} \right) (1 - c(T)) + \frac{1}{2} (1 + c(T)) \right) \right]. \end{aligned}$$

We proceeded in §3 by computing the roots of the partial derivative of the bound with respect to ρ . The same approach applies here, but unfortunately it does not lead to explicit expressions. However, a simple modification makes the bound more manageable. We write

$$\cos(x) = \frac{1}{2}(e^{ix} + e^{-ix}).$$

Since the argument of the cosine for $\rho > 1$ is purely imaginary, with positive imaginary part, the second exponential dominates the first. Hence, for large ω , we may approximate $B(\omega, n, \rho, T)$ by

$$\begin{aligned} \tilde{B}(\omega, n, \rho, T) &:= \frac{1}{\rho^n} \exp \left[\omega T \cosh^{-1} \left(\frac{1}{4} \left(\rho + \frac{1}{\rho} \right) (1 - c(T)) + \frac{1}{2} (1 + c(T)) \right) \right]. \end{aligned} \quad (23)$$

One can then explicitly find roots of the partial derivative of \tilde{B} with respect to ρ . We have

$$\begin{aligned} \rho^*(n) &= - \frac{n^2(c(T) + 3) + \omega^2 T^2(c(T) - 1) \pm 2n\sqrt{\omega^2 T^2(c(T)^2 - 1) + 2n^2(c(T) + 1)}}{\omega^2 T^2(c(T) - 1) + n^2(1 - c(T))}. \end{aligned} \quad (24)$$

These two roots are again each other's inverse. One quickly verifies that the square root is real and positive if and only if

$$n \geq \frac{1}{2} \omega T \sqrt{2 - 2c(T)} = \frac{1}{2} \omega r(T), \quad (25)$$

with

$$r(T) := T \sqrt{2 - 2c(T)}. \quad (26)$$

If this condition is satisfied, selecting the + sign in (24) yields the root that is greater than 1.

A little care is necessary when applying the bound (23). Recall that $f_2(u)$ is only analytic in Bernstein ellipses $e(\rho)$ with $\rho < E(T)$. It may be the case that $\rho^*(n) \geq E(T)$ and therefore we cannot use this bound directly. However, explicit computation yields the condition

$$E(T) \geq \rho^*(n) \quad \Leftrightarrow \quad n \geq \frac{2}{\sqrt{6+2c(T)}}\omega T. \quad (27)$$

Moreover, if $r(T)$ is given by (26), then

$$\frac{1}{2}r(T) < \frac{2}{\sqrt{6+2c(T)}}T, \quad \forall T > 1,$$

since $c(T) \in (-1, 1]$. With this to hand, we are now able to distinguish between the following cases:

1. $n < \frac{1}{2}\omega r(\mathbf{T})$. In this case the argument of the square root in (24) is negative and, hence, both roots are imaginary. The function $\tilde{B}(\omega, n, \rho, T)$ is either monotonically increasing or decreasing as a function of ρ on $[1, \infty)$. Reasoning as before, note that

$$\left. \frac{\partial \tilde{B}}{\partial \rho} \right|_{\rho=1} = \frac{1}{2}\omega r(T) - n. \quad (28)$$

The partial derivative vanishes precisely when $n = \frac{1}{2}\omega r(T)$ and it is positive for smaller n . Thus, the bound is increasing and the best possible bound we can find of the form (16) is

$$|a_n| \leq \tilde{B}(\omega, n, 1, T) = 2, \quad n < \frac{1}{2}\omega r(T).$$

2. $\frac{1}{2}\omega r(\mathbf{T}) < n < \frac{2}{\sqrt{6+2c(\mathbf{T})}}\omega \mathbf{T}$. In this case the argument of the square root in (24) is positive. Moreover, the condition $n < \omega T$ ensures that the overall expression for both roots ρ^* is positive (note that the denominator switches sign at $n = \omega T$). Thus, there is a minimum of $\tilde{B}(\omega, n, \rho, T)$ at $\rho = \rho^*(n) > 1$, and this minimum satisfies $\rho^*(n) < E(T)$. Therefore, we obtain the bound

$$|a_{n+k}| \leq \frac{2M_{\rho^*(n)}}{(\rho^*(n))^{n+k}} \leq \frac{1}{(\rho^*(n))^k} \tilde{B}(\omega, n, \rho^*(n), T) \leq \frac{2}{(\rho^*(n))^k}, \quad \forall k \in \mathbb{N}.$$

Hence, we deduce exponential decay of the coefficients a_n once n exceeds $n > \frac{1}{2}\omega r(T)$.

3. $\frac{2}{\sqrt{6+2c(\mathbf{T})}}\omega \mathbf{T} < n < \omega \mathbf{T}$. The arguments of the previous case still hold, but now $\rho^*(n) \geq E(T)$. Thus, the minimum value of $\tilde{B}(\omega, n, \rho, T)$ is obtained at $\rho = E(T)$ and therefore

$$|a_n| \leq \frac{2}{E(T)^n} \exp[\omega T \cosh^{-1}(2 + c(T))]. \quad (29)$$

Note that this bound is valid for all $n \in \mathbb{N}$, not just n in the stated range. However, it only gives an accurate portrait of the coefficient decay once n exceeds $\frac{2}{\sqrt{6+2c(T)}}\omega T$.

4. $n > \omega T$. The denominator of (24) vanishes at $n = \omega T$ and switches sign for larger n , so that $\rho^*(n)$ becomes negative. Based on (28), we may conclude that the bound is monotonically decreasing as a function of ρ on $[1, \infty)$. Once more we are limited to choosing $\rho \leq E(T)$, and therefore the estimate (29) is also applicable in this case.

This derivation establishes the resolution constant $r(T) = T\sqrt{2-2c(T)}$, but only for even oscillations $f(x) = \cos \omega \pi x$. To prove the complete result, we need to obtain an equivalent statement for the odd functions

$$f(x) = \sin \omega \pi x. \quad (30)$$

We proceed along similar lines to the cosine case. First, note that the Fourier extension of (30) equates to the orthogonal polynomial expansion of

$$f_2(u) = \frac{\sin \left[\omega T \cos^{-1} \left(\frac{u}{2}(1-c(T)) + \frac{1}{2}(1+c(T)) \right) \right]}{\sqrt{1 - \left[\frac{u}{2}(1-c(T)) + \frac{1}{2}(1+c(T)) \right]^2}}, \quad u \in [-1, 1].$$

It is not immediately apparent that this function is analytic at $u = 1$. However, simple analysis reveals that the square-root type singularity is removable, and consequently $f_2(u)$ is analytic in any Bernstein ellipse $e(\rho)$ with $\rho < E(T)$.

Proceeding as before, we find that the n th Chebyshev polynomial coefficient of $f_2(u)$ admits the bound $|a_n| \leq B(\omega, n, \rho, T)$, $\forall \rho > 1$, where

$$B(\omega, n, \rho, T) = \frac{2 \sinh \left[\omega T \cosh^{-1} \left(\frac{1}{4}(\rho + \frac{1}{\rho})(1-c(T)) + \frac{1}{2}(1+c(T)) \right) \right]}{\rho^n \sqrt{C(\rho, T)}},$$

and $C(\rho, T) = \left[\frac{1}{4}(\rho + \frac{1}{\rho})(1-c(T)) + \frac{1}{2}(1+c(T)) \right]^2 - 1$. Suppose first that $n < \frac{1}{2}\omega r(T)$. Letting $r \rightarrow 1^+$, we find that

$$|a_n| \leq \lim_{r \rightarrow 1^+} B(\omega, n, \rho, T) = 2\omega T.$$

Next suppose that $\frac{1}{2}\omega r(T) < n < \frac{2\omega T}{\sqrt{6+2c(T)}}$. Then, for sufficiently large ω , we can replace $B(\omega, n, \rho, T)$ by

$$\frac{\tilde{B}(\omega, n, \rho, T)}{\sqrt{C(\rho, T)}},$$

where $\tilde{B}(\omega, n, \rho, T)$ is the bound (23) of the cosine case. Hence, we deduce that

$$\begin{aligned} |a_{n+k}| &\leq \frac{2}{(\rho^*(n))^k \sqrt{C(\rho^*(n), T)}} \\ &= \frac{2}{(\rho^*(n))^k} \sqrt{\frac{n^2 - \omega^2 T^2}{2(1+c(T))n^2\omega^2 T^2 + (c(T)^2 - 1)\omega^4 T^4}}, \quad \forall k \in \mathbb{N}. \end{aligned}$$

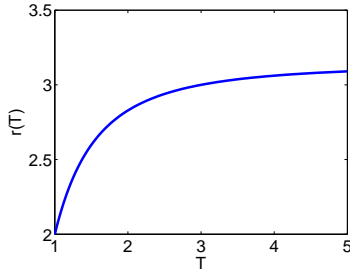


Figure 4: The resolution constant of Fourier extensions as a function of T .

Note that the square root term is bounded since $n > \frac{1}{2}\omega r(T)$. Indeed, it attains its maximal value at $n = \frac{1}{2}\omega r(T) + 1$, and hence is both bounded in n and ω . Therefore, this confirms exponential decay of the coefficients a_n for $n > \frac{1}{2}\omega r(T)$.

In the third scenario, i.e. $n > \frac{2\omega T}{\sqrt{6+2c(T)}}$, we use the value $\rho = E(T)$ to give

$$|a_n| \leq \frac{2}{(E(T))^n} \frac{\sinh[\omega T \cosh^{-1}(2 + c(T))]}{\sqrt{(2 + c(T))^2 - 1}}.$$

Note the similarity of this bound with (29) for the cosine case.

To sum up, we have shown the following:

Theorem 4.2. *The resolution constant $r = r(T)$ of the exact Fourier extension g_n is precisely $T\sqrt{2 - 2c(T)}$. In particular, $r(T) \sim 2$ for $T \approx 1$ and $r(T) \sim \pi$ for $T \gg 1$.*

The resolution constant $r(T)$ is illustrated as a function of T in Fig. 4. In Fig. 5 we further illustrate the theorem with several numerical examples. As discussed in §2.3, the result of the numerical computation of (3) may not coincide with the exact solution g_n . We shall discuss the question of resolution power of the numerical solution, as opposed to the exact solution, in detail in §4.2. For the moment, so that we can illustrate Theorem 4.2, we have removed this issue by carrying out computations in additional precision.

As shown in the right panel of Fig. 5, the resolution constant $r(T) \sim \pi$ for $T \gg 1$. The fact that $r(T)$ is independent of T for large T can be seen by the studying the quantity $f_2(u)$. For fixed ω and large T , we find that

$$f_2(u) = \cos\left(\frac{\pi\omega}{\sqrt{2}}\sqrt{1-u}\right) + \mathcal{O}(T^{-2}).$$

The leading term is independent of T , thus we expect $r(T)$ to approach a constant value as $T \rightarrow \infty$. It is also natural to expect that this constant is the same as the resolution constant of polynomial approximations. Indeed, for large T the functions $\cos \frac{\pi}{T}kx$ and $\sin \frac{\pi}{T}kx$ are not at all oscillatory on $[-1, 1]$. In particular, they are well approximated on $[-1, 1]$ by their Taylor series. As such, the span of the first n such functions is very close to the span of their Taylor series, which is exactly the span of polynomials. Thus, for fixed n and sufficiently large T , the Fourier extension g_n of an arbitrary function f closely resembles the best

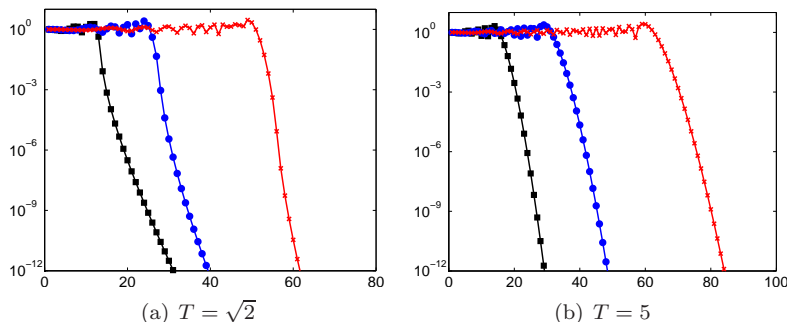


Figure 5: The error $\|f - g_n\|_{L^\infty_{[-1,1]}}$, where $f(x) = \exp(i\pi\omega x)$ and $\omega = 10, 20, 40$ (squares, circles and crosses respectively).

polynomial approximation to f in the L^2 sense; in other words, the Legendre polynomial expansion. The value of π for the resolution constant arises from the discussion in §3.

As commented at the start of this section, oscillations at ‘periodic’ frequencies $\omega = \frac{m}{T}$, $m \in \mathbb{Z}$, are informative in that they illustrate when the Fourier extension behaves roughly like a classical Fourier series on $[-T, T]$, that is, when $T \approx 1$, and when it does not, i.e. $T \gg 1$. The decay of the coefficients a_n for these oscillations is also quite special. Since $f(x) = \exp(i\frac{m}{T}\pi x)$ is entire and periodic on $[-T, T]$, the corresponding function $f_2(u)$ given by (21) is also entire in the variable u . This means that $f_2(u)$ is analytic in any Bernstein ellipse $e(r)$, and hence the corresponding Chebyshev coefficients a_n (respectively, the errors $\|f - g_n\|$) decay superexponentially fast, as opposed to merely exponentially fast at rate $E(T)$. Comparison of the left and right panels of Fig. 5 exemplifies this difference. We now summarize this observation along with the other convergence characteristics derived above in the following corollary to Theorem 4.2:

Corollary 4.3. *The error $\|f - g_n\|$ in approximating $f(x) = \exp(i\pi\omega x)$ is $\mathcal{O}(1)$ for $n < \frac{1}{2}\omega r(T)$. Once n exceeds $\frac{1}{2}\omega r(T)$ the error begins to decay exponentially. For $\omega = \frac{m}{T}$, $m \in \mathbb{Z}$, convergence is superexponential. Otherwise, whenever $n > \frac{2}{\sqrt{6+2c(T)}}\omega T$, the rate of exponential convergence is precisely $E(T)$.*

4.2 Resolution power of numerical approximations

As mentioned, it is not necessarily the case that the result of any numerical implementation will coincide with the exact Fourier extension. Therefore, the predictions of Theorem 4.2 may not be witnessed in computations. In Fig. 6 we give numerical results for the two numerical implementations discussed in §2.3, namely, the Galerkin and collocation methods. For small T there is little difference to the left panel of Fig. 5 (except, as mentioned in §4.2, the Galerkin method only attains around eight digits of accuracy). However, when $T \gg 1$ the numerical method appears to possess a much larger resolution constant than the value $r(T) \sim \pi$ predicted by Theorem 4.2. In fact, as demonstrated in Fig. 7, it appears that the numerical Fourier extension has a resolution constant of $2T$ for all T , much like the naïve estimate given at the start of §4.1. This observation

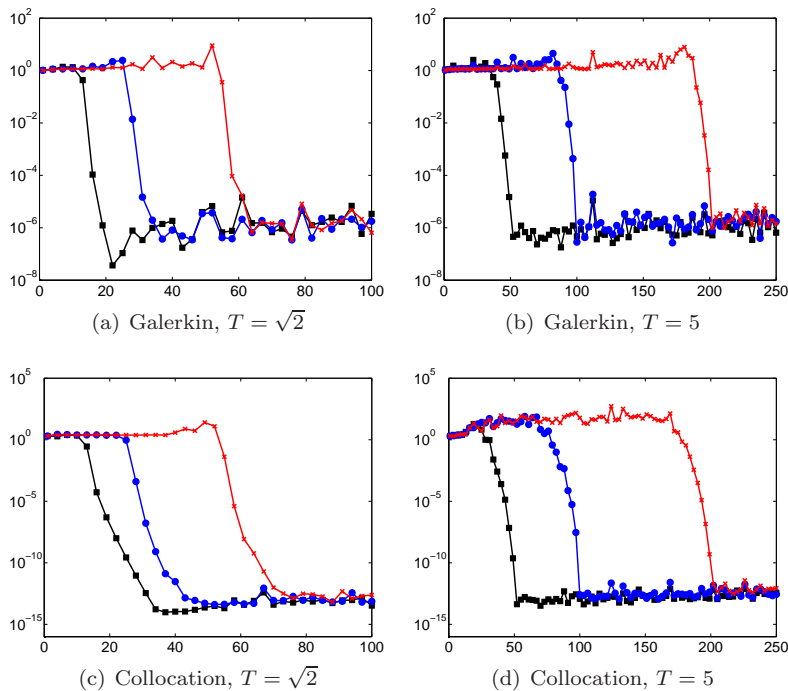


Figure 6: The error $\|f - g_n\|_{L^\infty_{[-1,1]}}$, where $f(x) = \exp(i\pi\omega x)$ and $\omega = 10, 20, 40$.

is further corroborated in Fig. 8, where a linear dependence of the numerical resolution constant with T is witnessed.

This difference can be explained intuitively. The improvement of Theorem 4.2 over the naïve estimate of §4.1 revolves around the observation that slowly oscillatory functions in the frame can be recombined to approximate functions with higher frequencies with exponential accuracy. This is due to the redundancy of the frame. However, such combinations necessarily yield large coefficients. Indeed, the orthogonal polynomials that yield the exact solution grow rapidly outside $[-1, 1]$ (see [19]) and, hence, their coefficients when represented in the frame consisting of exponentials that are bounded on $[-T, T]$ must be large. The numerical solution favours representations in the frame with bounded coefficients, since for large n the system becomes underdetermined and most least squares solvers will seek a solution vector with minimal norm (see [19]). One may conclude that while the resolution power of the frame is bounded by π , the resolution power of all representations in the frame with ‘reasonably small’ coefficients is only $2T$.

4.3 Fixed T versus varying T

Whilst the principal issue highlighted in the previous section, namely, that for large T we witness $r(T) \approx 2T$ rather than $r(T) \approx \pi$, is unfortunate, it is mainly the case $T \approx 1$ that is of interest, since this gives the highest resolution power.

Unfortunately, with T fixed independently of n , the resolution constant

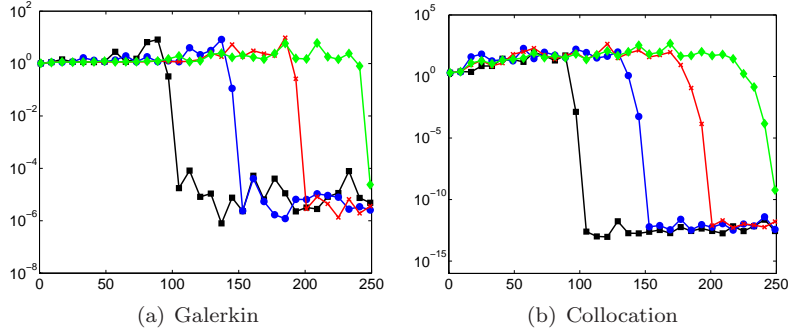


Figure 7: The error $\|f - g_n\|_{L^\infty_{[-1,1]}}$, where $f(x) = \exp(50i\pi x)$ and $T = 2, 3, 4, 5$ (squares, circles, crosses and diamonds respectively).

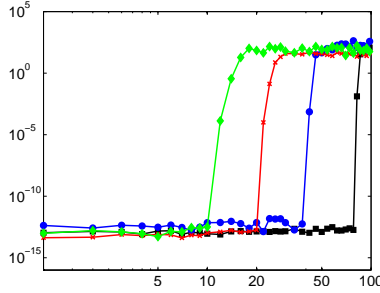


Figure 8: The error $\|f - g_{160}\|_{L^\infty_{[-1,1]}}$ against $\omega = 1, 2, \dots, 100$, where $f(x) = \exp(i\omega\pi x)$ and $T = 2, 4, 8, 16$ (squares, circles, crosses and diamonds respectively).

$r(T) > 2$; in other words, below that of the optimal Fourier estimate. One way to formally obtain the value of 2 is to allow $T \rightarrow 1$ with increasing n . Indeed, if

$$T = 1 + \frac{c}{n^\alpha},$$

for some $c > 0$ and $0 < \alpha < 1$, then we find that

$$r(T) = 2 + \frac{2c}{n^\alpha} + \mathcal{O}(n^{-2\alpha}) \rightarrow 1, \quad n \rightarrow \infty.$$

The disadvantage of such a choice of T is that one forfeits exponential convergence. In fact,

$$E\left(1 + \frac{c}{n^\alpha}\right) = 1 + \frac{c\pi}{n^\alpha} + \mathcal{O}(n^{-2\alpha}),$$

and therefore

$$E\left(1 + \frac{c}{n^\alpha}\right)^{-n} \sim \exp(-c\pi n^{1-\alpha}), \quad n \rightarrow \infty,$$

which indicates subexponential decay of the error (yet still spectral).

Another potential choice is to set $\alpha = 1$ (in which case, the above analysis breaks down). However, this leads to even worse convergence: namely, of order $n^{-\frac{1}{2}}$. Indeed, we have

Lemma 4.4. *Suppose that $T = 1 + \frac{c}{n^\alpha}$ with $1 \leq \alpha < 2$ and that $f \in H^1[-1, 1]$. Then, for some constant $c > 0$ we have*

$$\|f - g_n\|_{L^2_{[-1,1]}} \leq cn^{\frac{\alpha}{2}-1} \|f\|_{H^1_{[-1,1]}}.$$

Proof. Suppose that we extend f linearly outside $[-1, 1]$ to a function \tilde{f} which is periodic on $[-T, T]$ and continuous. Let \tilde{f}_n be the Fourier series of \tilde{f} on $[-T, T]$. Arguing as in the proof of Theorem 2.1, we find that

$$\|f - g_n\|_{L^2_{[-1,1]}} \leq \|\tilde{f} - \tilde{f}_n\|_{L^2_{[-T,T]}} \leq cn^{-1} \|\tilde{f}'\|_{L^2_{[-T,T]}},$$

for some $c > 0$. Since \tilde{f} is linear on $[-T, -1]$ and $[1, T]$ we have that $\tilde{f}'(x) = \mathcal{O}(n^\alpha)$ for $x \in [-T, T] \setminus [-1, 1]$. Therefore,

$$\|\tilde{f}'\|_{L^2_{[-T,T]}} \leq \|f'\|_{L^2_{[-1,1]}} + \sqrt{T-1} \|\tilde{f}'\|_{L^\infty_{[-T,T]}} \leq \|f'\|_{L^2_{[-1,1]}} + cn^{\frac{\alpha}{2}} \|f\|_{H^1_{[-1,1]}},$$

as required. \square

One can ask whether the convergence estimate predicted by this lemma is sharp. However, numerical experiments confirm this result. In particular, given that the value with $\alpha = 1$ corresponds precisely to the convergence rate of the standard Fourier series of a nonperiodic function f on $[-1, 1]$, there is no advantage gained in either convergence rate or resolution power from a Fourier extension with $T = 1 + \frac{c}{n^\alpha}$, $1 \leq \alpha < 2$. If one insists on a formal resolution constant of 2, but still rapid convergence, then it is best to use a parameter value $0 < \alpha < 1$. We will compare various choices of α and a fixed T in the following section.

4.4 Numerical experiments

In this final section we present numerical results for the Fourier extension method applied to the oscillatory functions

$$f_1(x) = (1 + x^2) \cos 10x \cos 100\pi x, \quad f_2(x) = \text{Ai}(-36x - 32), \quad (31)$$

where $\text{Ai}(z)$ is the Airy function. Graphs of these functions are given in the top row of Fig. 9.

In the second row of Fig. 9 we present the error committed by the Fourier extension for various choices of T . The convergence rates predicted in the previous section are confirmed for these examples. For T decreasing with n the oscillations are resolved slightly sooner, but there is slower convergence in the resolved regime. Whether the approximation error is better or worse than that obtained from a fixed value of T (in this case $T = \frac{4}{3}$) depends on what level of accuracy is desired. Yet, even when high accuracy $\epsilon \ll 1$ is required, $\alpha = 2/3$ (i.e. $T = 1 + \frac{1}{n^{2/3}}$) appears to be a good choice for these two examples.

As discussed, one motivation for using Fourier extensions is that, as rigorously proved in this paper, they offer a higher resolution power than polynomial

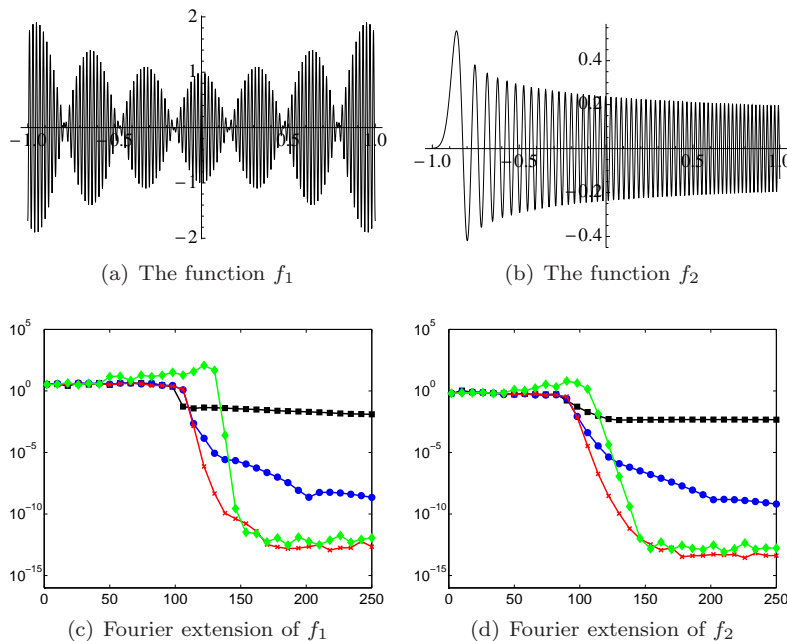


Figure 9: The top row shows the functions f_1 and f_2 defined by (31). The bottom row gives the error $\|f - g_n\|_{L^\infty[-1,1]}$, where $T = 1 + \frac{1}{n}$ (squares), $T = 1 + n^{-\frac{2}{3}}$ (crosses), $T = 1 + n^{-\frac{1}{2}}$ (circles) and $T = \frac{4}{3}$ (diamonds).

approximations, for which the resolution constant is π (see §3). In Fig. 10 we compare the behaviour of the Chebyshev expansion and the Fourier extension approximation for the functions (31). Note that the latter resolves the oscillatory behaviour using fewer degrees of freedom, in agreement with the result of §4. Indeed, for the first example function f_1 shown in the left panel, the Chebyshev expansion only begins to converge once n exceeds 150 (here, for purposes of comparison, the number of expansion coefficients is $2n$), in agreement with a resolution constant of π . Additionally, the resolution constant $r(T) \approx 2T$ (since T is small in this example) for the Fourier extension is also confirmed by Fig. 10.

The results for the second function f_2 are shown in the right panel of Fig. 10. The differences in resolution are smaller in this case. The choice $T = 4/3$ is comparable to using a Chebyshev expansion. Yet, the fixed choice $T = 8/7$ and varying choices of T still require significantly fewer degrees of freedom than the Chebyshev expansion for comparable accuracy. The choice $\alpha = 1/2$ leads to better results than $\alpha = 2/3$ in this example, but it is comparable to the fixed value $T = 8/7$. Note that the oscillations of f_2 are not harmonic, with the frequency increasing towards the right endpoint of the approximation interval. This seems to have the effect of reducing the advantage of schemes with better resolution properties.

Finally, we would like to note that using different solvers may lead to slightly different numerical results, as different solvers have different ways of treating very ill-conditioned problems. All examples of finite precision in this paper, including both Galerkin and collocation discretizations, were produced using

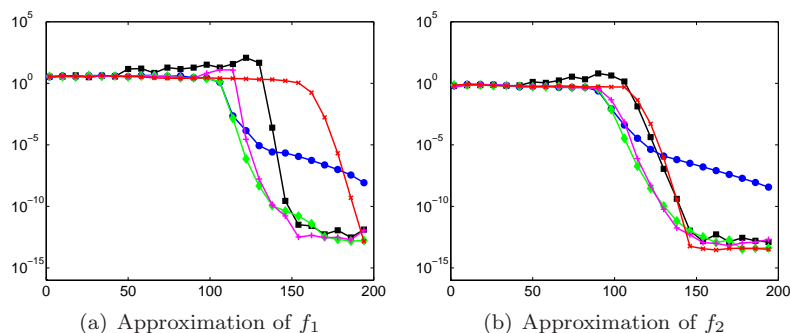


Figure 10: The error $\|f - g_n\|_{L^{\infty}[-1,1]}$, where g_n is Chebyshev expansion (crosses), or the Fourier extension approximation with $T = \frac{4}{3}$ (squares), $T = 1 + n^{-2/3}$ (circles), $T = 1 + n^{-1/2}$ (diamonds) and $T = \frac{8}{7}$ (plus).

the backslash operator of Matlab 7.

References

- [1] R. A. Adams. *Sobolev Spaces*. Academic Press, 1975.
- [2] N. Albin and O. P. Bruno. A spectral FC solver for the compressible Navier–Stokes equations in general domains I: Explicit time-stepping. *preprint*, 2011.
- [3] A. Averbuch, M. Israeli, and L. Vozovoi. Analysis and applicaion of Fourier–Gegenbauer method to stiff differential equations. *SIAM J. Num. Anal.*, 33(5):1844–1863, 1996.
- [4] J. P. Boyd. *Chebyshev and Fourier Spectral Methods*. Springer–Verlag, 1989.
- [5] J. P. Boyd. A comparison of numerical algorithms for Fourier Extension of the first, second, and third kinds. *J. Comput. Phys.*, 178:118–160, 2002.
- [6] J. P. Boyd. Fourier embedded domain methods: extending a function defined on an irregular region to a rectangle so that the extension is spatially periodic and C^{∞} . *Appl. Math. Comput.*, 161(2):591–597, 2005.
- [7] J. P. Boyd and J. R. Ong. Exponentially-convergent strategies for defeating the Runge phenomenon for the approximation of non-periodic functions. I. Single-interval schemes. *Commun. Comput. Phys.*, 5(2–4):484–497, 2009.
- [8] O. Bruno and M. Lyon. High-order unconditionally stable FC-AD solvers for general smooth domains I. Basic elements. *J. Comput. Phys.*, 229(6):2009–2033, 2010.
- [9] O. P. Bruno, Y. Han, and M. M. Pohlman. Accurate, high-order representation of complex three-dimensional surfaces via Fourier continuation analysis. *J. Comput. Phys.*, 227(2):1094–1125, 2007.

- [10] E. J. Candès. Compressive sampling. In *Proceedings of the International Congress of Mathematicians, Madrid, Spain*, pages 1433–1452, 2006.
- [11] C. Canuto, M. Y. Hussaini, A. Quarteroni, and T. A. Zang. *Spectral methods: Fundamentals in Single Domains*. Springer, 2006.
- [12] O. Christensen. *An Introduction to Frames and Riesz Bases*. Birkhauser, 2003.
- [13] K. S. Eckhoff. On a high order numerical method for functions with singularities. *Math. Comp.*, 67(223):1063–1087, 1998.
- [14] D. Gottlieb and S. A. Orszag. *Numerical Analysis of Spectral Methods: Theory and Applications*. Society for Industrial and Applied Mathematics, 1st edition, 1977.
- [15] D. Gottlieb and C.-W. Shu. Resolution properties of the Fourier method for discontinuous waves. *Comput. Methods Appl. Mech. Engrg*, 116:27–37, 1994.
- [16] D. Gottlieb and C.-W. Shu. On the Gibbs’ phenomenon and its resolution. *SIAM Rev.*, 39(4):644–668, 1997.
- [17] D. Gottlieb, C.-W. Shu, A. Solomonoff, and H. Vandeven. On the Gibbs phenomenon I: Recovering exponential accuracy from the Fourier partial sum of a nonperiodic analytic function. *J. Comput. Appl. Math.*, 43(1–2):91–98, 1992.
- [18] N. Hale and L. N. Trefethen. New quadrature formulas from conformal maps. *SIAM J. Numer. Anal.*, 46(2):930–948, 2008.
- [19] D. Huybrechs. On the Fourier extension of non-periodic functions. *SIAM J. Numer. Anal.*, 47(6):4326–4355, 2010.
- [20] A. J. Jerri. The Shannon sampling theorem – its various extensions and applications: A tutorial review. *Proc. IEEE*, 65(1565–1596), 1977.
- [21] D. Kosloff and H. Tal-Ezer. A modified Chebyshev pseudospectral method with an $\mathcal{O}(N^{-1})$ time step restriction. *J. Comput. Phys.*, 104:457–469, 1993.
- [22] M. Lyon and O. Bruno. High-order unconditionally stable FC-AD solvers for general smooth domains II. Elliptic, parabolic and hyperbolic PDEs; theoretical considerations. *J. Comput. Phys.*, 229(9):3358–3381, 2010.
- [23] R. Pasquetti and M. Elghaoui. A spectral embedding method applied to the advection–diffusion equation. *J. Comput. Phys.*, 125:464–476, 1996.
- [24] T. Rivlin. *Chebyshev Polynomials: from Approximation Theory to Algebra and Number Theory*. Wiley New York, 1990.
- [25] L. N. Trefethen. Is Gauss quadrature better than Clenshaw-Curtis? *SIAM Rev.*, 50(1):67–87, 2008.